Journal of Applied Polymer Science

Relations between Structure and Property of Polyamide 11 Nanocomposites based on Raw Clays Elaborated by Water-Assisted Extrusion

Gregory Stoclet,[1] Michel Sclavons,[2] Jacques Devaux[2]
[1]Unité Matériaux Et Transformations, CNRS UMR 8207, Université de Lille1, 59655 Villeneuve d'Ascq, France
[2]Bio-and Soft Matter (BSMA), Institute of Condensed Matter and Nanosciences (IMCN), Université Catholique de Louvain (UCL), B-1348 Louvain-la-Neuve, Belgium
Correspondence to: G. Stoclet (E-mail: gregory.stoclet@univ-lille1.fr)

ABSTRACT: Bio-based polymers and polymer nanocomposites have known an increasing interest during the past few years. This work is focused on the elaboration and the characterization of bio-based nanocomposites made from polyamide 11 (PA11) and nonorgano-modified montmorillonite. To elaborate these materials an original elaboration process, consisting in injecting water during the extrusion, was used. Results show that thanks to this process, a well exfoliated morphology is obtained for clay contents as high as 10% wt. This was explained on the one hand by the fact that the clay is soluble in water and on the other hand by the fact that water and PA11 are miscible at high pressure and high temperature. Moreover, the morphology analyses have revealed that from 10% wt of clay, the platelets were not totally randomly distributed but they were rather organized at a mesoscopic scale. The obtaining of such clay's dispersion involves an enhancement of thermomechanical properties. For example, for a clay content of 10% wt, the Young's modulus of the material can be doubled and its degradation temperature increased. The role of the elaboration conditions on the morphology and subsequent properties of the nanocomposites are also carefully analyzed. Finally, it has been evidenced that the presence of the filler infers on both the crystalline form induced and the crystallization kinetics. In summary, this study demonstrates that, in the case of PA11 nanocomposites, the water-assisted injection process leads to the achievement of an exfoliated morphology for clay contents as high as 10% wt that allows to obtain high performance materials and to be free from using organomodified clays.

KEYWORDS: nanocomposite; water assisted extrusion; Polyamide 11; exfoliation

Received 7 March 2012; accepted 13 May 2012; published online
DOI: 10.1002/app.38053

INTRODUCTION

Polymer nanocomposites are a broad class of materials knowing an increasing interest from both academicals and industrial researchers. The main goal of compounding polymeric resins with fillers is to drastically enhance material property with adding small amount of filler.[1–6] Among this, broad class of materials polyamide 6 (PA6)/montmorillonite (MMT) nanocomposites have attracted much interest since the pioneering works first developed by Toyota research group.[7–10] Besides, in the case of PA6, it has been shown that adding a few percent of filler drastically enhance mechanical properties, especially the Young's modulus,[1–7] improve heat-distortion temperature[1–5] (HDT), and confers both good barrier[8] and fireproof properties.[9] Surprisingly even if PA6 nanocomposites has been largely studied and found to be a good matrix for the elaboration of nanocomposites and as an excellent clay dispersion can be achieved, there are few studies dealing with nanocomposites based on other polyamides used as matrix. Among the broad polyamide family, polyamide 11 (or nylon11) has known a growing interest in recent years, for one due to its bio-based character. Besides PA11 is an important commercial polyamide known for its excellent piezoelectricity properties[11,12] which can be better than the ones of polyvinyldiene difluoride (PVDF) at elevated temperatures.[13] This polymer is used in a large range of industrial fields from automotive to offshore applications[14–17] despite of its relatively poor mechanical properties. Indeed even if PA11 exhibits a higher elongation at break and Izod impact than PA6, its elastic modulus and yield strength are lower.[18] Regarding to structural aspects, PA11 is a polymorphic polymer that exhibits at least five crystalline forms which are largely dependent on

both thermal history and processing conditions.[19–22] With the aim of improving the PA11 performances, particularly the mechanical ones, PA11-based nanocomposites have recently been the focuses of a large number of studies.[23–33] Regarding their processing, nanocomposites based on PA11 can be obtained by either in-situ methods or by the melt intercalation technique. In this way it has been largely demonstrated that an *in situ* elaboration method generally leads to a good dispersion state of the clay platelets into the matrix but is not suitable for large-scale production. On the other hand, melt blending is a more environmentally friendly and industrially viable method for producing nanocomposites even if the dispersion state achieved is generally poorer. Furthermore, it has been largely shown that the elaboration of polymer nanocomposites based on raw fillers generally leads to the formation of microcomposites with poor properties, due to the poor affinity existing between the polymer and the filler. As a consequence, to compensate the dispersion loss using the melt blending route, fillers are generally organomodified. The goals of this chemical modification are first the improvement of the affinity with the matrix and second the increase of the distance between the stacked clay platelets, this in order to get access to a better dispersion state.

In this way most of the studies dealing with PA11 nanocomposites have been devoted to the elaboration and the characterization of PA11 filled with organomodified MMT using different elaboration routes. For example, PA11/MMT nanocomposites have been prepared and characterized by Zhang et al. by means of *in situ* polymerization.[34] The authors show first that when using this method it was possible to obtain fully exfoliated nanocomposites at low clay loading (i.e. 4% wt) while a mixture of exfoliated and intercalated was obtained for higher clay contents. Moreover, they show that thermal properties and crystallization behavior were enhanced in the case of nanocomposites. Finally they also point out that the dispersion state achieved is better when using an organoclay as compared with neat clay. On the other hand, Liu et al. prepared PA11 organomodified MMT nanocomposites using the melt blending route.[35] They report the same behavior as Zhang et al., i.e. the elaboration of an exfoliated morphology for clay contents below or equal to 4% wt and a mixture of both exfoliated and intercalated clays for higher filler contents. Regarding the influence on the material properties, authors report a drastic increase of both modulus and thermal stability in opposition with a decrease of both the elongation at break and glass transition temperature. For example, using the same elaboration route, Hu et al. reported an increase of the elastic modulus of about 30% in the case of PA11 filled with 5% wt of organomodifed clay.[36]

To summarize, a review of the literature shows that, in the case of PA11 nanocomposites, a good dispersion of the clays is achieved, and thus an improvement of properties is obtained, only when an organomodified filler is used. On the other hand, the few articles devoted to studies of PA11 nanocomposites based on untreated clays have shown that a poor dispersion state is achieved resulting in a material with low performances. Indeed regarding the use of unmodified clays rather than organomodified ones, Bur et al. report that the extent of exfoliation in the case of PA11/neat MMT nanocomposites elaborated by melt blending no exfoliation was obtained.[37] This relies in the fact that the neat layered silicates show poor interactions with organic polymers. Moreover, in the case of untreated clays, the intercalation of the polymer chains between the platelets is very difficult due to the small distance, about 1 nm, between the stacked platelets. Therefore, nanoscale structures are mostly obtained by dispersion of organically modified layered mineral clays [most often montmorillonite (MMT)]. Nevertheless, the organic modification of MMT suffers a few drawbacks. First, because of the high surface area, a large ratio modifier/clay (sometimes in the range 30%–50% by weight) is required. Moreover, the organic modification is thermally rather unstable, limiting polymer processing to temperatures below 200°C and finally the full process remains rather expensive.[3] As a consequence, succeed in the elaboration of nanocomposites based on raw MMT can be of prime interest, especially in the case of PA11 in order to "keep the green character" of such materials. Moreover, the elaboration of these green nanocomposites seems possible as previous works have shown that well-exfoliated PA6 nanocomposites based on nonorganically modified clays can be elaborated using a special melt blending route.[38] This method, consisting in injecting water during the extrusion process, has been successfully used and shown in the case of PA6/MMT nanocomposites, where well-exfoliated platelets of MMT were obtained resulting in a properties enhancement of the material.[38,39] Basically, water injection is supposed to compensate the low affinity between matrix and raw clay and to act as a surfactant. Moreover, in the case of PA6 it has been shown that injecting water induces a solubilization of the polymer when both a critical water content and a critical pressure are reached.

As a consequence this study is devoted to the elaboration and the characterization of PA11 nanocomposites based on nonorganomodified clays using the water-assisted extrusion route. Particularly, the effect of injecting water during the process on the nanocomposites morphology and properties has been carefully studied. To reach this goal, series of PA11 nanocomposites having different clay contents have been elaborated under different conditions with and without the injection of water during the extrusion process. Their nanoscale and mesoscale morphologies as well as structural, thermal, and mechanical properties have been characterized in order to assess the role of the injection of water during the process and to establish the relations between structure and properties.

EXPERIMENTAL

Materials

The polyamide 11 used in this study is an injection grade (BMNO TLD) supplied by Arkema under the tradename Rilsan®. The sodium modified montmorillonite (NaMMT) clay was supplied by Southerm Clay Products and will be denoted as MMT for sake of clarity. This kind of clay consists in a pristine MMT which has just been washed in order to remove most of the impurities. Another type of clay, to know a Raw MMT, has also been used. Raw MMT is a nonpurified bentonite, mainly made of NaMMT but also containing nonsmetic products such as quartz, mica, feldspar,… Contrary to pristine NaMMT, which

Table I. Elaboration Conditions Used

Temperature (°C)	Material throughput (kg/h)	Screws speed (rpm)	Water input (mL/min)	Clay throughput (% wt)
190°C	6 and 20	200 and 1000	0 and 50	0, 5, 10, and 20

only contains smectic clay after chemical treatment, the latter silicate is not washed. Pristine refers to NaMMT, whose purification step from bentonite includes the use of surfactants but is not considered as a modification. Before processing, PA11 pellets were dried during 24 h at 50°C under a primary vacuum in order to remove moisture traces. As PA11 is highly sensitive to the presence of moisture, the clays were also dried during 24 h at 100°C under the same vacuum.

The PA11 nanocomposites were elaborated by melt blending in a corotating twin-screw extruder Coperion Mega Compounder WP ZSK25 ($L/D = 40$). Water, when used, was pumped into the extruder in the high compression zone. The special design of the screw allows the pressure to increase up to 125 bars in this zone which prevents water evaporation. The water is degassed in the transport zone and fully removed using a vacuum pump. The processing temperature (°C), the throughput (TP), the screws speed (SP), and the water injection rate (W) were adapted to the experience. A more detailed description of this process is available elsewhere.[40,41] The elaboration conditions used in this study are listed in Table I.

Nanocomposites filled with clay contents varying from 0% to 20%wt have been elaborated. The sample with 20% wt is elaborated with the future aim of predispersing the clay into the matrix and to serve as a masterbatch. Structural and morphological characterizations were performed on the as extruded pellets. The properties determination was carried out on compression molded samples from 0.5 mm thick sheets molded at 190°C under 90 bars. Before compression molding, pellets were dried at 50°C under vacuum during 12 h.

SAXS and WAXS Analyses

Wide angle X-ray scattering (WAXS) and small angle X-ray scattering analyses were carried out owing to a Genix microsource (XENOCS) equipment operating at 50 kV and 1 mA. The Cu-K_α radiation used ($\lambda = 1.54$ Å) was selected with a curved mirror monochromator. WAXS and SAXS patterns were recorded on a two-dimensional CCD VHR camera (Photonic science) the distance between sample and detector (D) being set at $D = 7$ cm for WAXS and $D = 80$ cm for SAXS. The working distance was calibrated using PE sample and silver behenate standards for WAXS and SAXS, respectively. Standard corrections such as distortion, dark current subtraction, and background correction were applied before analysis. The two-dimensional WAXS patterns obtained were then azimuthally integrated using the fit2D software.

Morphology Analyses

Morphologies of the nanocomposites were characterized by means of both optimal microscopy (OM) and transmission electronic microscopy (TEM). The images to illustrate the dispersion of filler were obtained by means of a binocular optical microscope Ceti STEDDY T equipped with a numerical camera Nikon COOLPIX 4500. Examinal area of the produced composites was prepared from a 500 µm thin film cut from the elaborated pellets using a razor blade. Micrographs of the samples were taken under magnitude of 10 to provide an actual visual aspect of the samples. Clay dispersion and exfoliation degree were examined by means of TEM. The TEM micrographs were recorded using LEO 922 (Zeiss) transmission electron microscope operating at 200 kV. Analyzed samples were thin films, having thickness of approximately 70 nm, microtomed from bulk samples at room temperature using a Leica Reichert FCS microtome and collected on a 300-mesh copper grid.

Thermal Properties

Differential scanning calorimetric (DSC) analyses were carried out on a Perkin Elmer DSC7 apparatus in order to determine the characteristic temperatures of samples. The equipment was calibrated using an Indium standard using standard procedures. About 10 mg samples, inserted into aluminum pans, were analyzed from 20°C to 220°C at heating and cooling rates of 10°C/min under nitrogen environment.

A high pressure differential scanning calorimetric (HPDSC) Mettler Toledo HPDSC 827_e (maximum pressure: 100 bars) was used in order to study the phases separation or miscibility of PA11 and water at high pressure and high temperature. The measuring chamber is connected to a pressure controlling valve (Brooks P.C. 5866 series) regulated by a Brooks valve controlled (Reads Out & Control Electronic 0152). Thanks to this device, pressure and temperature can be independently set in the DSC oven and the heating/cooling curves measured at constant pressure, allowing the simulation of the processing conditions. In order to reproduce the conditions within the extruded PA11 and water were blended at a weight ratio of 50/50, the full sample weighing was around 10 mg. PA11 pellets were freeze-ground in a grinding device (Pulverisette 14, Frisch) at 14,000 rpm.

The thermal stability of the materials was checked by thermogravimetric analyses (TGA, Mettler Toledo TGA/SDTA 851_e) under nitrogen atmosphere, from 200°C to 500°C at 5°C/min with a stabilization period of 2 min at 200°C. Samples weighing from 8 to 9 mg were die-cut in 1 mm cold-pressed pellet sample so as to keep constant dimensions and contact surface. The results are presented as temperature at 10% weight loss (T10) calculated above 200°C as the weight loss before this temperature is attributed to water evaporation. T10 is usually considered as the critical decomposition temperature. Each value is an average of minimum four experiments.

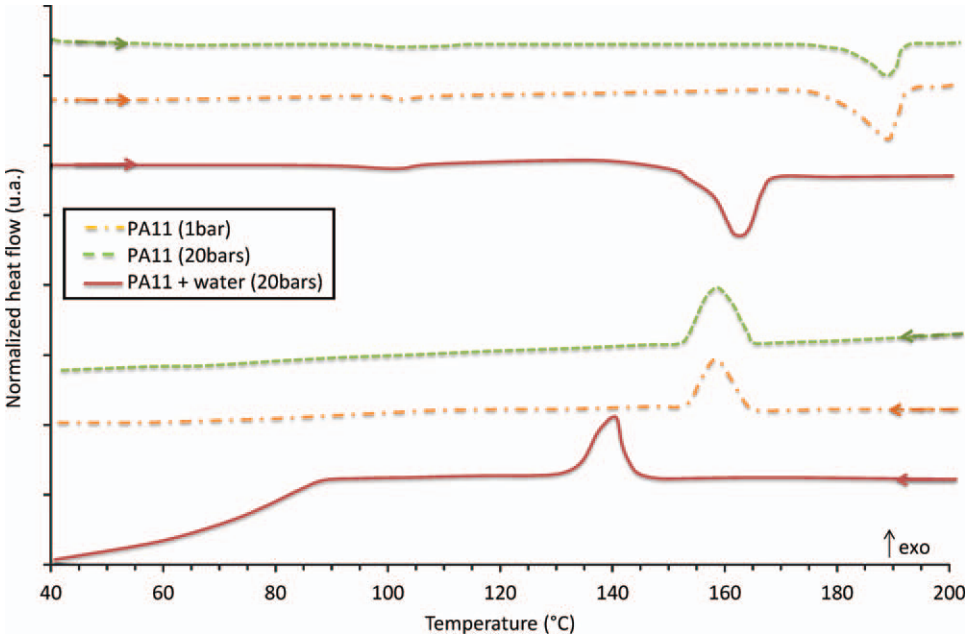

Figure 1. DSC thermograms of (a) neat PA11 at 1 bar, (b) neat PA11 at 20 bars, and (c) neat PA11 + water at 20 bars. [Color figure can be viewed in the online issue, which is available at wileyonlinelibrary.com.]

Mechanical Properties

Mechanical behaviors were determined by means of uniaxial tensile tests at room temperature (RT) using an INSTRON 4466 tensile machine. The dumbbell specimens having 22 mm and 5 mm in gauge length and width were strained at a constant crosshead speed of 12.5 mm/min, i.e. an initial strain rate $\dot{\varepsilon}^{\circ} = 0.01\ s^{-1}$. Five specimens were tested for each kind of samples.

Viscoelastic Properties

A RSA3 apparatus from TA Instrument was used for dynamic mechanical analysis (DMA). Experiments were performed at a frequency of 1 Hz in the temperature range 25 to 90°C. The dynamic strain amplitude, $\varepsilon^{o} = 0.4 \times 10^{-3}$, was determined after preliminary measurement of the strain domain for which the material obeys linear viscoelasticity.

RESULTS AND DISCUSSION

Polymer–Water Miscibility Characterization

Polyamides are well known for their hygroscopic nature, and almost all the relaxation processes are strongly affected by moisture level of the polymer specimens. The influence of water absorption on the various relaxations was largely studied.[42–44] Whatever the polyamide type it was found that water acts as a plasticizer of the polymeric system, and causes a significant depression in the T_g. For example, in the case of PA6, T_g shifts from 80°C in the case of dry PA6 to −10°C in the case of PA6 having a water content of 9% wt. More recently it has been also proposed that PA6 is soluble in water at elevated temperature and pressure.[45,46] A more precise comprehensive study recently published[47] has shown that minimum water concentration and applied pressure are required to achieve the PA6 dissolution. In addition, it appears that the PA6 miscibility with water greatly improves the dispersion of the clays into the matrix as shown by Touchaleaume et al. in the case of PA6 MMT nanocomposites.[38] Intuitively it can be expected that PA11 can also be miscible to water to. In order to confirm the latter, high-pressure DSC experiments have been carried out. Thermograms recorded upon heating and subsequent cooling are reported on Figure 1.

HPDSC thermograms indicate that while applying a hydrostatic pressure of 20 bars does not influence the thermal properties of PA11, the presence of a water excess in the same conditions strongly decreases both melting and crystallization temperatures of about 30°C. Hence, in the same way than for PA6, water and PA11 are partly miscible at elevated pressures and temperatures. The maximum solubility of water into PA11 can be estimated using the equations reported below which are taken from Ref. 47 and adapted to PA11:

$$\frac{n_{PA11}}{n_{H2O}} = \frac{2}{3} \rightarrow \frac{m_{PA11}}{m_{H2O}} = \frac{2}{3} \cdot \frac{183}{18} = \frac{183}{27}$$

$$\frac{m_{PA11}}{m_{sysy}} = \left(1 + \frac{m_{H2O}}{m_{PA11}}\right)^{-1} = 0.87$$

The calculation indicates that a maximum concentration of 13% wt of water is miscible in PA11. Regarding the extrusion parameters used in this study it appears that the concentration of water injected during the extrusion process is above this critical value. Indeed as indicated in Table II, at 1000 rpm the

Table II. Water Content for Extrusion Performed at 200 and 1000 rpm

Screw speed (rpm)	Feeding rate (g/min)	Water injection rate (g/min)	Water content (%)
200	33 g/min	50 g/min	150%
1000	83 g/min	50 g/min	40%

water/polymer ratio is equal to 40% wt while it is equal to 150% wt at 200 rpm.

This behavior is of prime interest considering that in the presence of water the PA11 macromolecules will be more mobile than in bulk. Thus it can be assumed that, as for PA6 nanocomposites, the macromolecules diffusion between the clay platelets is easier, which may lead to a better dispersion state.

Morphology and Structure Characterization

The efficiency of the clay platelets in reinforcing the polymer matrix is primarily determined by the degree of its dispersion into the matrix. As large aggregates of clay can be easily distinguishable by naked eyes in the samples with a lower degree of dispersion, a fine approach for a best comparison of the dispersion in different composites was given first by optical microcopy observations. Figure 1 shows the optical images of PA11 containing 5, 10, and 20% wt of clay extruded at 200 and 1000 rpm with and without water injection. The OM micrographs were carried out on a large number of samples and the micrographs reported on Figure 2 are representative of the morphology observed.

Without water injection it appears that whatever the clay content many aggregates having a micronic size are visible indicating a poor dispersion state even for low clay loadings. The micrographs obtained at 1000 rpm without water injection still exhibit a poor dispersion state even if the aggregates seem slightly smaller and fewer. On the other hand, when water is added during the extrusion process at 200 rpm, no more aggregates are visible at 5% wt and few, rare, and tiny aggregates could be still observed at 10% wt. This clearly demonstrates the positive effect of injecting water on the dispersion of the clays into the PA11 matrix. Moreover, it appears that a poorer dispersion state is observed when the screw speeds is increased and/or for high filler loadings.

Usually, high extrusions rates are recommended to increase shearing stresses to break down the clay aggregates (stacks) and finally to promote clay exfoliation. However, the latter is also dependant on the diffusion of the polymer matrix, thus on process duration. The intercalation is usually improved when a larger residence time is adopted. The observations by OM indicate already that under the process conditions, the residence time seems to have a more important effect on the quality of the dispersion than the shearing force. This fact has ever been pointed out by Bousmina who claimed that there's a compromise between the residence time and the shearing force in order to get access to a good dispersion state.[48]

In our case it appears that the water injection has a clearly more pronounced effect than both the shearing forces and the residence time. Indeed, on the one hand, if one compares the morphologies obtained at 200 rpm and 1000 rpm with a clay content of 5% wt; the morphologies observed are almost the same. Thus these two extrusion conditions seem similarly poor. In opposition, when water is added, the dispersion states are clearly better. Particularly the best dispersion is observed for low screw speeds.

In order to confirm the achievement of the complete dispersion-exfoliation of clay in the matrix, TEM observations were carried out. Figure 3 reports characteristic micrographs at different magnifications obtained for different processing conditions of PA11 filled with 5% wt of clays.

The composites containing 5% wt of clay processed at 200 rpm without water [Figure 3(b), 1000 rpm with water Figure 3(c) and without water Figure 3(d)] show that despite the presence of aggregates or microsized clay stacks observed previously, homogeneously distributed small few nanometers thick clay tactoids of several clay platelets and well-individualized clays layers randomly dispersed are observed. This is more pronounced especially when water is injected during the process. The best clay dispersion-exfoliation is observed with combining low extrusion rate and water injection [200 rpm with water (Figure 3(a)]. In this case, the clay platelets are homogeneously, randomly, individualized and distributed. These results demonstrate that exfoliated PA11/NaMMT nanocomposites can be obtained without requiring an expensive organomodification. This possibility to use unmodified clay has been reported in the case of PA6, PEBA clay nanocomposites, or PP clay nanotubes (halloysite) nanocomposites.[49] In this latter case, while a poor morphology was achieved for PP nanocomposites using conventional processing route, a good dispersion state was achieved for water-assisted extrusion. As previously discussed, this shows that in the present case injection of water has a greater positive effect than increasing the shearing forces or the residence time.

The influence of the filler content on the morphology was also investigated. For sake of clarity only the case of samples elaborated at 200 rpm with water injection will be discussed here. TEM micrographs obtained for different nanocomposites having clay contents varying from 5 to 20% wt are reported on Figure 4.

It is noteworthy to mention that the good clay dispersion previously observed with a clay concentration of 5% wt, is still preserved at higher clay loading (10 wt % NaMMT) as presented in Figure 3(b). For a clay content of 20% wt, in addition to isolated platelets, numerous tactoids, having slightly higher thicknesses that the ones observed at 5% wt composed of a stacking of several platelets are visible. Moreover, for 20% wt it appears that the fillers are rather oriented in the shear flow direction.

The global and local preceding observations have been completed by WAXS analyses to confirm the dispersion state determined from microscopy experiments. Exfoliation of clays is linked to the diffusion of the polymeric chains into the spaces between the clay galleries in view to surpass their cohesive forces by the hydrodynamic separation forces applied by the matrix in the molten state. Exfoliation is always preceded by intercalation which results from the diffusion of the polymer into the intergallery spaces of the clays. In this way, WAXS is of prime interest in order to quantify the intercalation degree. Moreover, the study of the crystalline structure of PA11 nanocomposites by means of XRD is also of prime interest for the understanding of the structure-property relationships. Figure 5 reports the two-dimensional WAXS patterns obtained for neat PA11 [Figure 5(a)] and PA11 filled with 5 wt % of NaMMT [Figure 5(b)] both extruded at 200 rpm with water injection.

Applied Polymer SCIENCE

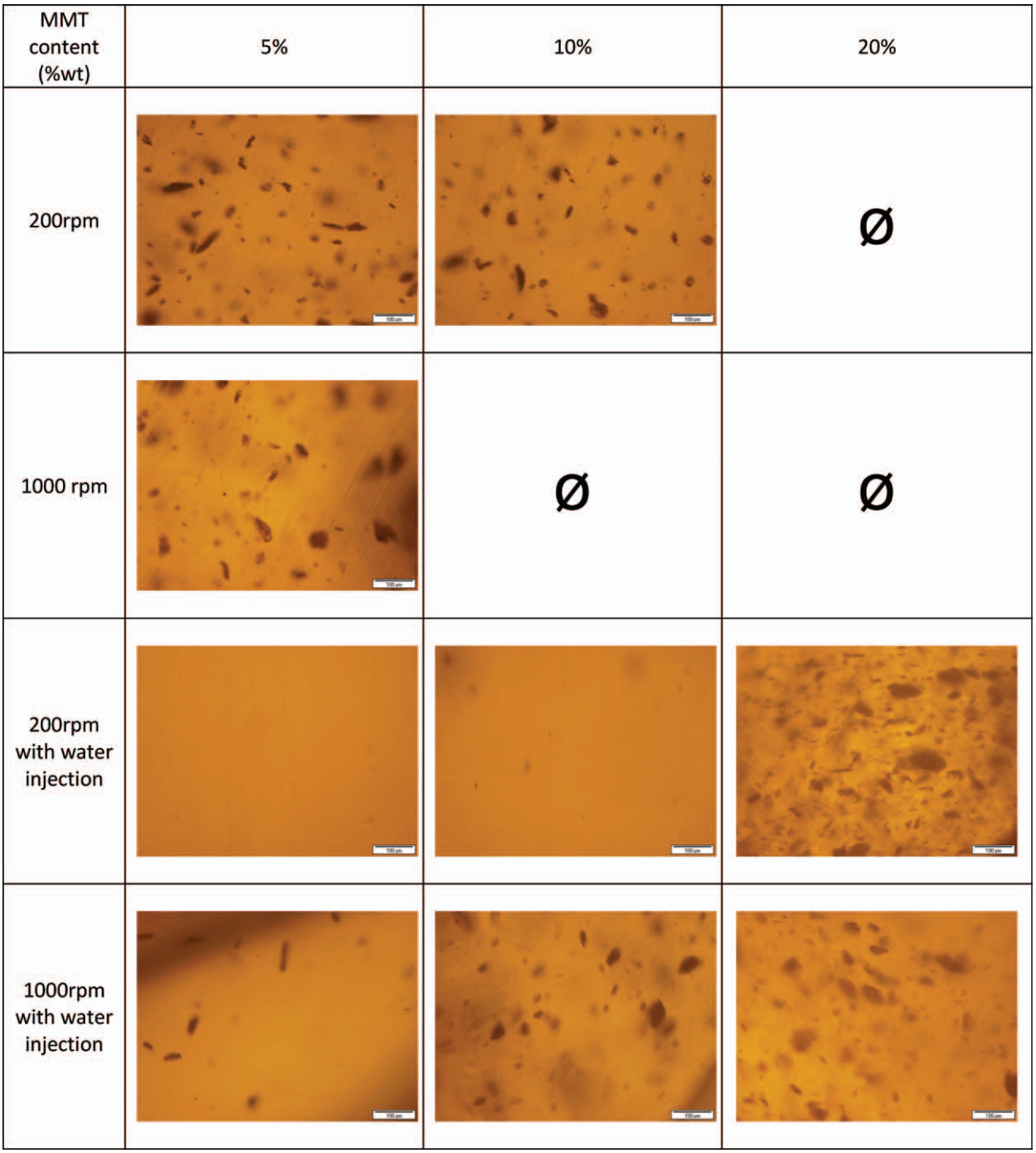

Figure 2. Microstructures of the PA11 composites elaborated under different conditions obtained by optical microscopy. [Color figure can be viewed in the online issue, which is available at wileyonlinelibrary.com.]

First the WAXS patterns show that in both case PA11 is semi-crystalline as revealed by the presence of (i) diffraction rings in the case of unfilled PA11 or (ii) the presence of diffraction arcs in the case of the nanocomposite. The presence of diffraction arcs rather than diffraction rings indicates that the nanocomposite has an oriented structure contrary to unfilled PA11. As the processing conditions being the same, this indicates that the presence of clays strongly promotes the orientation of the polymer chains along the flow direction. Moreover, at low angles, i.e. near from the beam stop, an intense scattering related to the diffusion by the clays is observed. This scattering is horizontally oriented indicated that the clays are rather oriented along the flow direction, in agreement with TEM observations.

In order to determine the crystalline phase(s) of PA11 involved, the intensity profiles were computed from the radial integration of the two-dimensional patterns. Figure 6 depicts the results obtained for samples elaborated using different conditions.

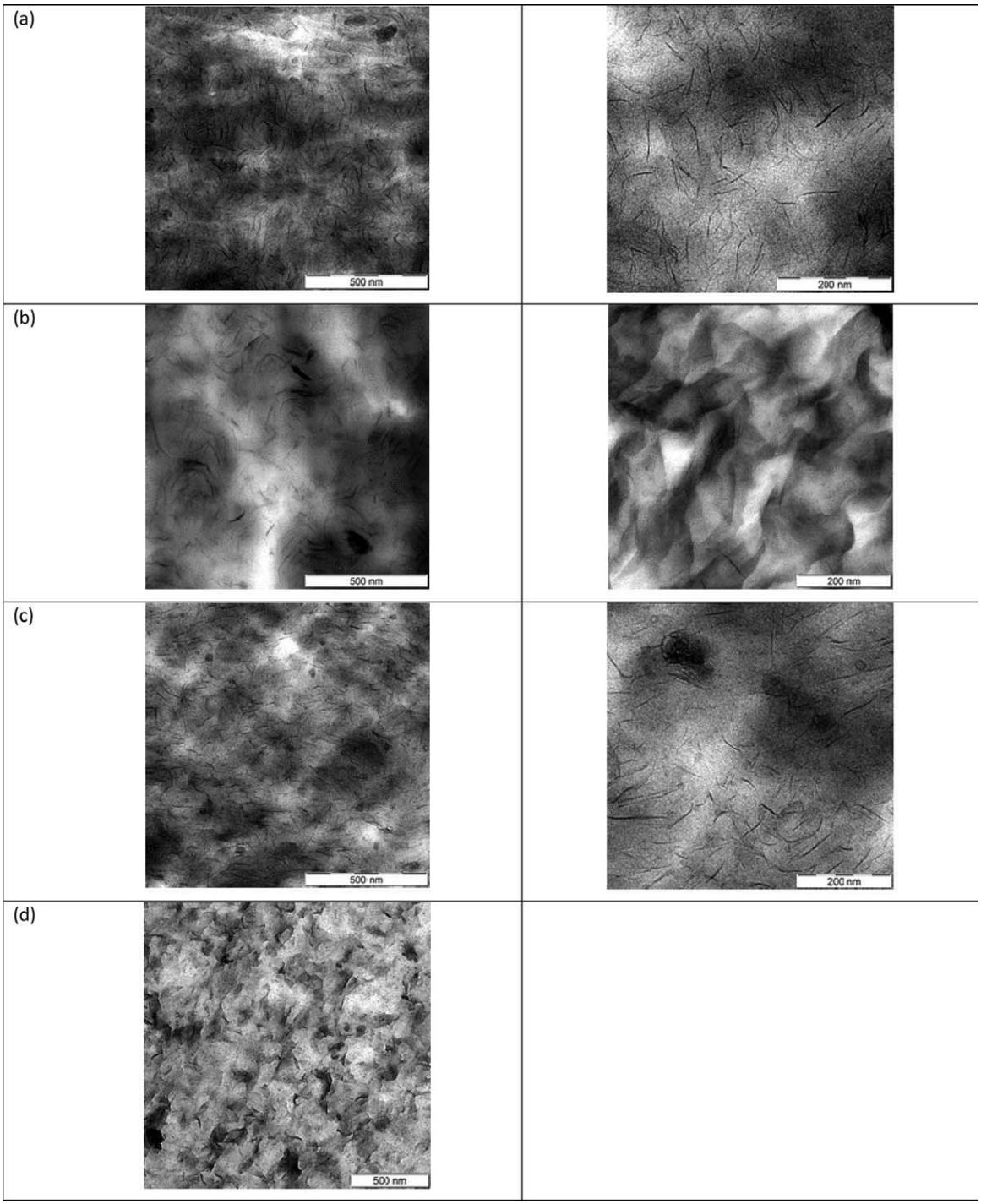

Figure 3. TEM micrographs of PA11 filled with 5% wt MMT processed at: 200 rpm (a) with water injection and (b) without water injection 1000 rpm (c) with water injection and (d) without water injection.

Regarding unfilled PA11 two diffraction peaks at $2\theta = 7^\circ$ and $2\theta = 22^\circ$ are observable. These peaks are characteristic of the γ crystalline form. On the other hand, in the case of nanocomposites, while the peak located at $2\theta = 7^\circ$ is still observable, two peaks rather than one are observable in the $19^\circ < 2\theta < 25^\circ$ region. These peaks at $2\theta = 21^\circ$ and $2\theta = 22.5^\circ$, respectively indicate that the crystalline α form is induced in the case of nanocomposites rather than the γ one. Nevertheless the two peaks are not clearly separated which means that the crystalline phase may be composed of a mixture of the γ and α ones. Previous studies have shown that the α form is more stable than the γ one.[50] This means that the presence of clay promotes the formation of the more thermodynamically stable crystalline form. The formation of the α form in the case of nanocomposites may be twofold. First, due to the nucleating effect of the clays the crystallization occurs at a higher temperature allowing

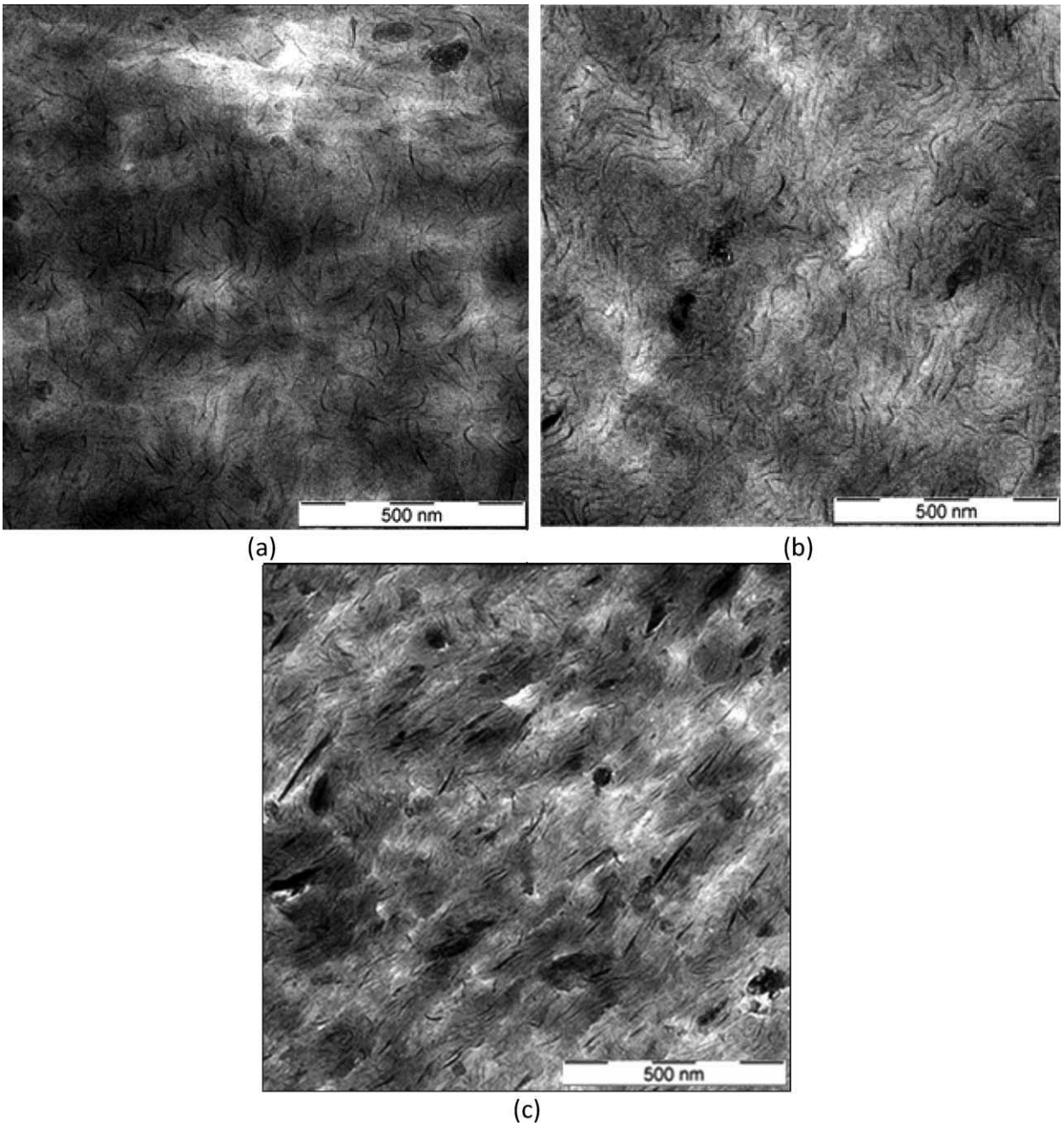

Figure 4. TEM micrographs of PA11 nanocomposites elaborated at 200 rpm with water injection having filler contents of (a) 5%, (b) 10%, and (c) 20%.

thus the formation of a more stable crystalline form. Second, one can envisage that, as for PA6, there are strong interactions between the clays surfaces and the PA11 chains which favor the formation of the α form rather than the γ one. Particularly, Zhang et al. have shown that the hydrogen bonds of PA11 are weakened upon addition of clay that restricts the formation of hydrogen bonding sheets by forcing the amide groups out of the hydrogen bonding sheets.[51] Moreover, VanDerHart et al. have shown by means of RMN experiments that, the γ-phase growth from the clay surface, obtains a head start on any growth of the α-phase originating in regions away from the clay surface.[52] This behavior will be discussed mater in the article.

Regarding the clay scattering, the intensity profile of pure MMT reported on Figure 6, exhibits a diffraction peak at $2\theta = 7.5°$ ascribed to the d_{001} diffraction plane of MMT, i.e. to the diffraction arising from the basal planes. This d_{001} value, equal to 1.18 nm, corresponds to the distance between two stacked platelets separated by one layer of water in the clay interlayer. It is worth noticing that this value is fairly lower than the ones reported in the cases of the organomodified clays usually used for the elaboration nanocomposites, which are generally around to 4 to 5 nm resulting in an easier exfoliation of the clay platelets. In other words in this case there are still high cohesive bonds between the platelets and as claimed by Bousmina, this

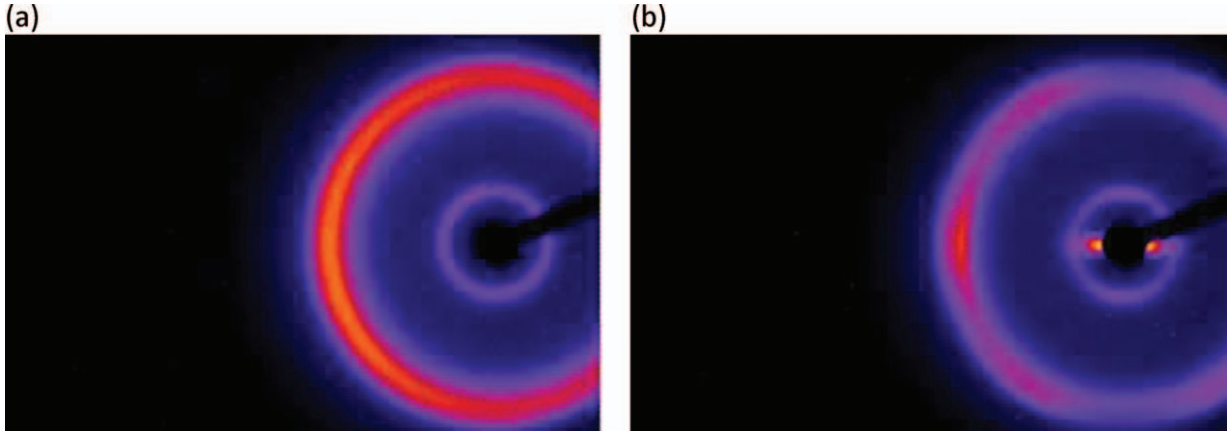

Figure 5. Two-dimensional WAXS patterns of (a) neat PA11 and (b) PA11 filled with 5% wt MMT elaborated both at 200 rpm with water injection (The shear flow direction is vertical). [Color figure can be viewed in the online issue, which is available at wileyonlinelibrary.com.]

interplatelets distance is unfavorable to their delamination.[48] For nanocomposites loaded with 5% wt and 10% wt of clays, no diffraction peak characteristic of the (001) plane of the clays is observable in the angular region analyzed. As this peak is characteristic of the regular stacking of clay platelets in the pristine clay, this shows that no or almost no tactoids are remaining in the materials. Nevertheless PA11 exhibits a diffraction peak around 7°, which corresponds as mentioned previously to the γ crystalline form. As a consequence it cannot be ascertained that there is no slight d_{001} diffraction hidden by the PA11 peak. However, an increase of the scattered intensity is observed in the low 2θ region. This increase is related to the scattering arising from isolated clay platelets and/or from a stacking of a limited number of platelets. It also appears that the more the clay content is the more intense this signal is. This means that even for high clay contents there's a significant part of isolated clays confirming the previously discussed TEM results. Nevertheless WAXS analysis does not clearly put in evidence an influence of the elaboration conditions used while the TEM analysis has highlighted that injecting water during the extrusion favors the exfoliation. For nanocomposites having a clay content of 20% wt a broad shoulder is observed at $2\theta = 5.5°$ and $2\theta = 6.5°$ for samples elaborated at 200 rpm and 1000 rpm, respectively. As this shoulder is located at angles smaller than the one observed for the neat clay, this means that an intercalation phenomenon has occurred. Particularly, the d_{001} value increase from 1.2 nm to 1.6 nm for samples elaborated at 200 rpm and 1000 rpm, respectively. This small increase indicates that the intercalation degree is very low. To go further in the characterization of the microstructure, and in order to know if the behavior observed

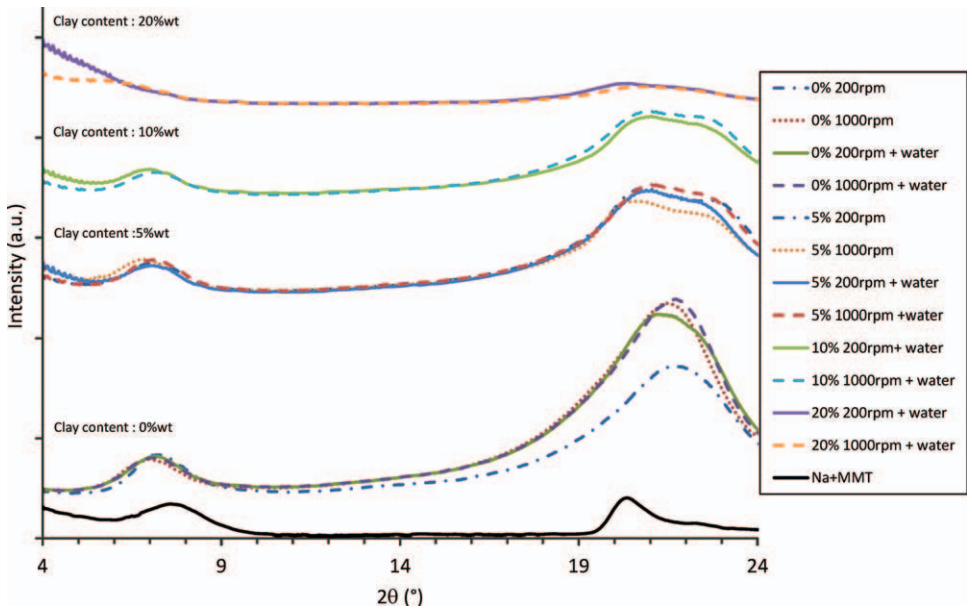

Figure 6. Integrated intensity profiles of PA11 samples elaborated using different conditions. [Color figure can be viewed in the online issue, which is available at wileyonlinelibrary.com.]

Applied Polymer SCIENCE

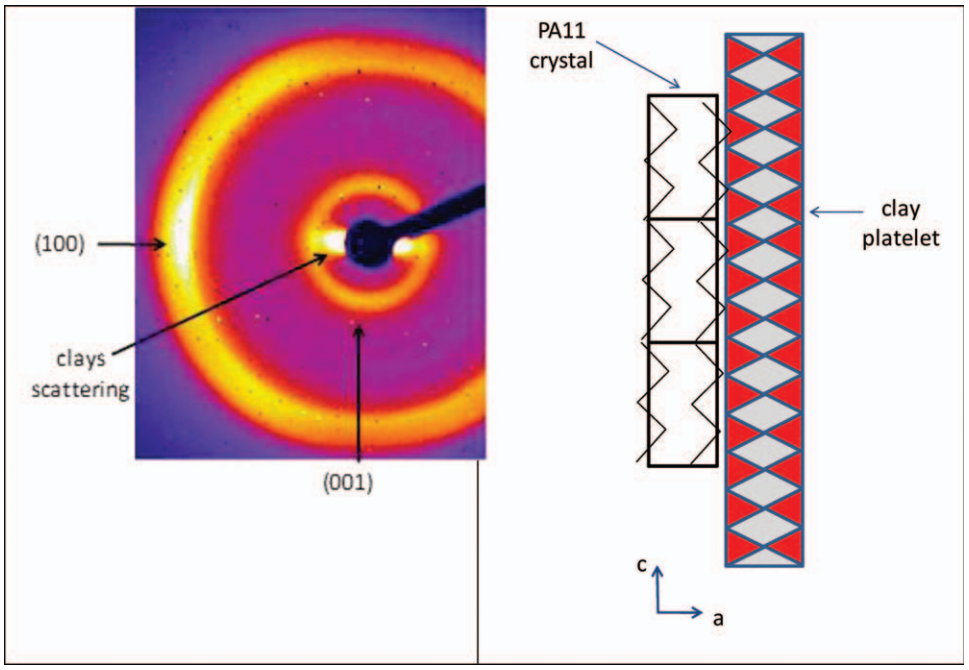

Figure 7. (a) Two-dimensional WAXS pattern of PA11 nanocomposite filled with 5% wt MMT elaborated at 1000 rpm with water injection and (b) schematic of the corresponding structure (the flow direction is vertical). [Color figure can be viewed in the online issue, which is available at wileyonlinelibrary.com.]

by VanDerHart in the case of PA6 is the same in PA11, two-dimensional WAXS patterns have also been analyzed in terms of orientation.

The two-dimensional WAXS pattern of a PA11 nanocomposite filled with 5% wt MMT elaborated at 1000 rpm with water injection is reported at Figure 7(a). On this pattern one can note that the diffraction arc related to the (001) diffraction plane (i.e. the peak at $2\theta = 7°$) is located in the polar region while the diffraction arc related to the (100) diffraction plane (i.e. the peak at $2\theta = 20°$) is in the equatorial region. This means that the PA11 crystals are mainly vertically oriented (in the landmark of the figure) or in other words that the crystals are oriented along the flow direction. The scattering signal arising from the clays shows that the MMT platelets are oriented along this direction too. Thus it appears that the crystals long axis is parallel to the clays surface as sketched on Figure 7(b). As a consequence it can be assumed that PA11 crystals are laid on the clays surface and thus that they have start to growth from the latter. As a consequence the same behavior than the one observed for PA6 can be envisaged here. Finally to support TEM observations, morphology of nanocomposites has been characterized by means of SAXS in order to highlight the organization at a mesoscale.

Figure 8 depicts the Lorentzian representation $Iq^2 = f(q)$ of the SAXS intensity profiles obtained for the nanocomposites elaborated at 200 rpm with water injection. On this Figure 8, two broad peaks are visible in the case of PA11 nanocomposite while only one appears in the case of unfilled PA11. The presence of a peak in this angular region is, in the case of semicrystalline polymers, ascribed to the presence of a long period (Lp) arising from the periodic alternation of crystalline and amorphous domains. Regarding this one can assume that the peak observed at $q = 0.8$ nm^{-1} for neat PA11 is ascribed to the PA11 long period which is equal to about 8 nm. This peak shifts from $q = 0.8$ nm^{-1} to $q = 0.6$ nm^{-1} when the clay content increases from 0 to 20% wt. This means that the long period, initially equal to 8 nm increases up to reach a value of 10.5 nm when 20% wt of filler is added. In other words the presence of clays involves the formation of larger organized domains despite the well-known confinement effect induced by the presence of clays. The origin of this phenomenon has not been clearly determined

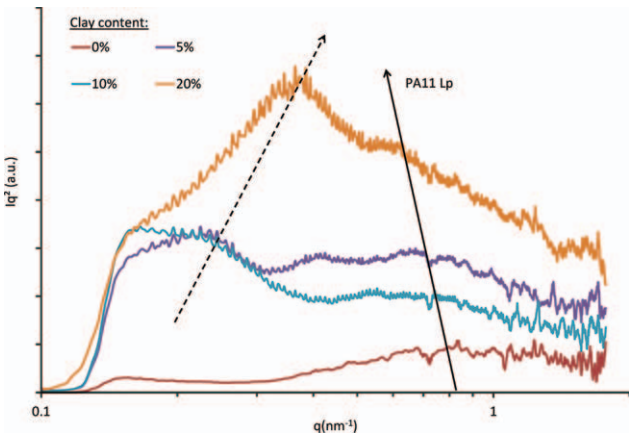

Figure 8. Lorentzian representation of the SAXS intensity profiles recorded for PA11 nanocomposites having different clay contents elaborated at 200 rpm with water. [Color figure can be viewed in the online issue, which is available at wileyonlinelibrary.com.]

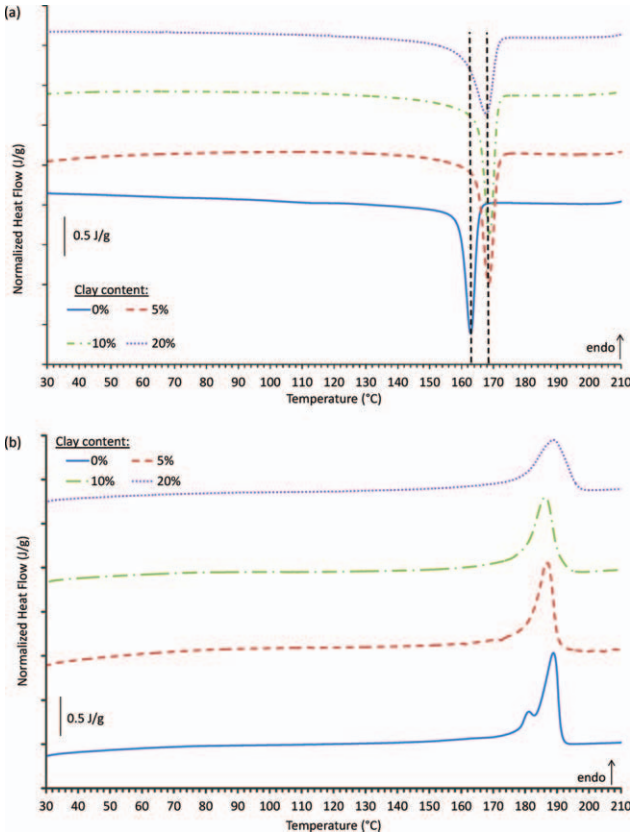

Figure 9. Thermograms of PA11 nanocomposites of different clay contents processed at 200 rpm with water injection recorded upon (a) cooling and (b) second heating. [Color figure can be viewed in the online issue, which is available at wileyonlinelibrary.com.]

in this study. In the case of nanocomposites an additional peak is observed at lower q. Regarding to this peak, which is observed only in the case of nanocomposites, it can be seen that it shifts from $q = 0.2$ nm^{-1} to higher q values as the clay content increases. Particularly for a clay content of 20% wt this peak is centered on $q = 0.36$ nm^{-1} which corresponds to a characteristic distance of 18 nm. A comparison of this value with the TEM observations tends to show that this peak is related to a mean distance between platelets. Indeed the TEM analysis (see Figure 1) has revealed that, particularly at high clay loading, platelets were not randomly distributed into the matrix but are rather parallel to each other at a quite constant interdistance. Moreover, the lower the clay content the higher this average interdistance. A question ensuing from this observation is to know if the presence of an interplatelets distance means that an intercalated structure has been formed or does it result from a mesoscale organization of the clays. First the measured distance, above 18 nm is far larger than the gyration radius of the polymer chains (5–6 nm) which means that several PA11 chains are enclosed between the platelets. Moreover, this distance is also far above the distance of 4 to 5 nm where the interactions between the platelets became weak. As a consequence the platelets can be considered as independent the ones to the others. Thus SAXS and TEM observations are relevant of a mesoscale organization of the clays.

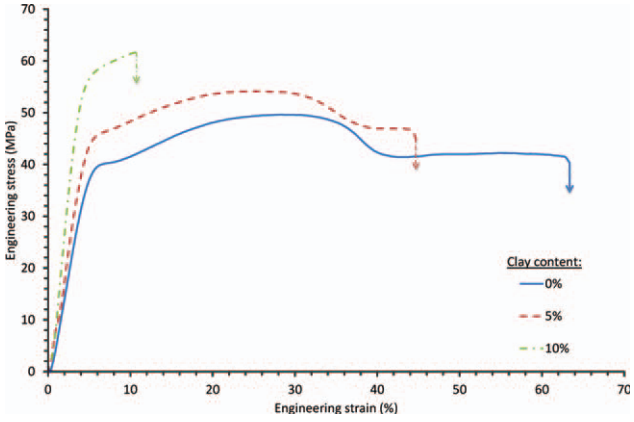

Figure 10. Engineering stress–strain curves obtained for PA11 nancomposites stretched at room temperature. [Color figure can be viewed in the online issue, which is available at wileyonlinelibrary.com.]

Thermal Properties Characterization

Quantifying the effect of clay nanofiller on the crystallization of the PA11 matrix is of prime interest as it directly influences the thermomechanical properties of the PA11. Figures 9(a, b) and 10 depicts the DSC thermograms recorded during cooling from the melt and subsequent heating, respectively for samples extruded with water injection at a screw speed of 200 rpm. The values of the cold crystallization temperature (T_c) and melting temperature (T_m) measured from these results are reported in Table III.

The thermograms recorded upon cooling indicate that T_c is about 5°C higher whatever the clay content in comparison from the one of unfilled PA11. The earlier start of the crystallization process means that the crystallization process is easier in the case of the nanocomposites indicating the nucleating effect of the clays. Contrary to the subsequent heating step, while a double melting peak is observed for neat PA11, only a single endotherm is present for nanocomposites with a broadening of this peak at high clay's concentration. The presence of a double melting peak observed in the case of PA11 can be ascribed to a melting-recrystallization process of the γ form into the stable α one. As the nanocomposites directly crystallize into the α-form it is obvious that no double melting peak is observed. The T_m broadening means a distribution of the crystal thicknesses broadening in regard of neat PA11 due to the confinement effect induced by the clay platelets.

Table III. Crystallization Rate as a Function of Clay Content for PA11 Nanocomposites Elaborated at 200 rpm with Water Injection

Clay content (% wt)	T_c (°C)	T_m (°C)
0	162.8	188.8
5	167.6	188.7
10	167.7	186.2
20	168.5	186.6

Applied Polymer SCIENCE

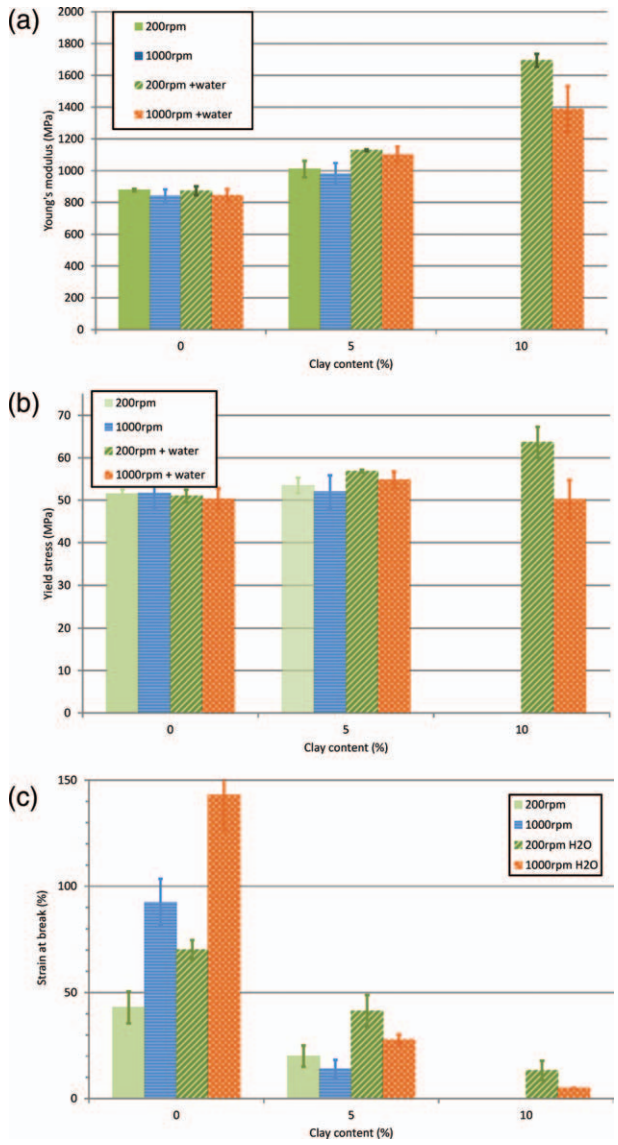

Figure 11. Evolution of (a) Young's modulus, (b) yield stress, and (c) elongation at break as a function of clay conditions for PA11 nanocomposites elaborated under different conditions. [Color figure can be viewed in the online issue, which is available at wileyonlinelibrary.com.]

Analysis of PA11/Clay Nanocomposites Mechanical Properties

Tensile Properties. It is well known that incorporating a filler into a polymer matrix infers on the resulting mechanical behavior. Particularly a sharp mechanical reinforcement is expected when clay platelets are well-dispersed into the polymer matrix. Figure 11 illustrates the mechanical behavior at room temperature (RT) for samples elaborated at 200 rpm with water injection as a function of the clay content.

As can be seen, in the case of unfilled PA11, the deformation occurs in three stages. The first stage, occurs until $\varepsilon = 5\%$, and corresponds to the viscoelastic domain where the stress sharply increases with increasing strain. It is followed by a homogeneous plastic deformation stage, for $5 < \varepsilon < 30\%$, during which the nominal strain slightly increases with increasing deformation. In this deformation range both the amorphous phase and the crystalline phase deforms uniformly. Finally up to $\varepsilon = 30\%$ a necking phenomenon occurs, showing that the deformation becomes heterogeneous, until sample's break. In the case of PA11 nanocomposites it can be observed that increasing the clay content implies an increase of both the yield stress and the Young's Modulus. Regarding the strain at break, the decrease induced by the presence of 5% wt of clay is quite limited. This is surprising considering that the presence of a filler is known to drastically embrittle the material. On the other hand for the nanocomposite filled with 10% wt a sharp decrease of the strain at break is observed. This behavior is currently encountered when nanoparticles are added into a polymer matrix. An explanation can be found in the decrease of the molecular mobility induced by the presence of the filler that involves a lack of deformability of the polymer within the interphase close to the particle. Moreover, these variations may be attributed to the differences in the dispersion state of the clays. Indeed while for 5% wt the morphology is fully exfoliated, a significant number of aggregates are present for 10% wt of clays. It is probably this aggregates which are responsible of the embrittlement of the material as they act as stress concentrations points. Figure 11 reports the evolution of Young's modulus, Yield stress and elongation at break respectively for PA11/clay nanocomposites extruded at 200 and 1000 rpm with and without water injection.

Results reported on Figure 11(a) show the evolution of the Young's modulus as a function of the draw conditions. Whatever the elaboration conditions, an increase of the Young's modulus is observed with increasing the clay content. Particularly it is worth noticing that for the PA11 nanocomposite elaborated at 200 rpm with water injection and filled with 10% wt of MMT the Young's modulus is increased by a factor of 2 as compared with the unfilled polymer extruded in the same conditions. This increase is noticeable and comparable to the one reported by Liu et al. in the case of well-dispersed PA6-MMT nanocomposites[53] or for PA11-organomodified MMT nanocomposites.[54] Regarding the influence of the elaboration conditions, for nanocomposites filled with 5% wt of MMT, it appears that the Young's modulus is slightly lower for materials elaborated at 1000 rpm. This may arises from overheating at high screw speeds which promotes polymer thermal degradation. Regarding to the effect of water injection it can be seen that there's no significant influence on unfilled PA11 while the Young's modulus of the nanocomposites elaboration without water injection are lower of about 10% than the ones measured for nanocomposites elaborated with water injection. This can be explained by the differences in the clays dispersion state previously highlighted as it is known that the higher the exfoliation degree is the higher the Young's modulus value. In opposition, for a clay content of 10% wt, increasing the shear rate clearly has a negative effect on the value of the Young's modulus. Indeed the value for the sample elaborated at 1000 rpm is 18% lower than the one measured for the sample at 200 rpm. In the same way than for the effect of injecting water at 5% wt of clay, this difference arises from a poorer dispersion state for the nanocomposite elaborated at 1000 rpm. Regarding to the Yield stress

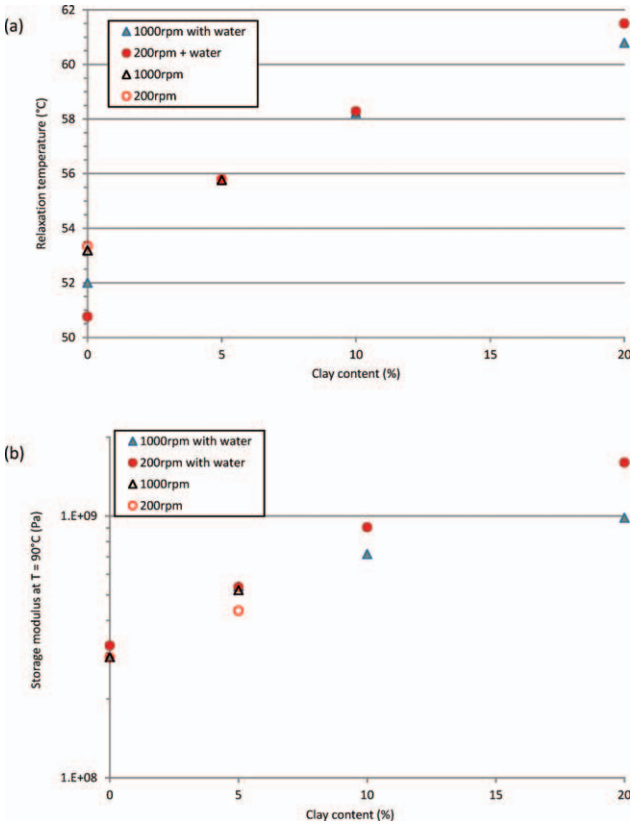

Figure 12. Evolution of (a) relaxation temperature and (b) storage modulus at 90°C as function of clay content for samples elaborated under different conditions. [Color figure can be viewed in the online issue, which is available at wileyonlinelibrary.com.]

evolution [Figure 11(b)], the same conclusions than for the Young's modulus can be drawn. The Yield stress increases of about 15 Mpa when 10% wt of MMT is added to PA11. It confirms the efficiency of the water injection associated with a sufficient residence time to obtain PA11 nanocomposites with improved mechanical properties. The evolution of the elongation at break reported on Figure 11(c) is more difficult to interpret as it strongly depends on the elaboration conditions used. A general trend is that the elongation at break is higher for samples extruded with water injection. This can be explained by the fact that the water injection involves a plasticization of PA11 which may hinder thermal degradation. Elongation at break of PA11/NaMMT prepared with water decrease with increasing clay content but not so dramatically when 5% wt of clay is processed at low shear rate in presence of water.

Viscoelastic Properties. The viscoelastic properties of the materials have been investigated. Only the α relaxation temperature and the viscoelastic properties in the rubbery state will be discussed. The corresponding results are reported on Figure 12.

The clay content increases the relaxation temperature T_α whatever the elaboration conditions used. Particularly for samples elaborated at 200 rpm with water injection, this temperature shifts from 52°C in the case of neat PA11 to 62°C when 20% wt of MMT is added. The T_α increase is generally ascribed to a decrease of molecular mobility into the polymer. In this case it can be ascribed to the confinement effect induced by the presence of platelets. The molecular mobility decrease observed in this study emphasizes the nucleating effect of the clays. Indeed even if macromolecules are less mobile, the crystallization kinetics are faster in the case of nanocomposites. Regarding the storage modulus in the rubbery state, the same behavior than the one observed for the Young's modulus is observed namely a sharp increase of the rubbery modulus with increasing the clay content whatever the elaboration conditions and the samples elaborated at 200 rpm with water injection exhibit the better properties improvement.

Thermal Stability

Finally to complete the properties characterization, thermal stability of PA11 and its nanocomposites elaborated at 200 rpm has been assessed. Higher thermal stability is commonly observed when clay platelets are well dispersed into the polymer matrix, as a result of limited oxygen supply, hindered out diffusion of the volatile decomposition products and also of char formation that acts as physical barrier between the polymer and the oxidative medium. The evolution of the degradation temperature T10 as a function of the clay content is reported on Figure 13.

First, for neat PA11, the degradation temperature T10 is located around 393°C and is not significantly influenced by the injection of water during the extrusion. Regarding to the influence of incorporating clay, a sharp increase of T10 is observed when the clay content is increased. Particularly a shift of 35°C is observed for PA11 filled with 10% wt of clay extruded with water. Such a shift amplitude has been previously reported by Liu et al. but at lower clay content. Indeed in their study, authors report a 35°C at a clay content of a few percent but a sharp decrease of the degradation temperature for clay contents above 5% wt.[35] This difference with the results of the present study may be explained first by the differences in the dispersions states achieved but also by the fact that in their studies, Liu et al. use an organomodified clay and thus the presence of a surfactant may decrease T10 the thermal stability.[35] It also

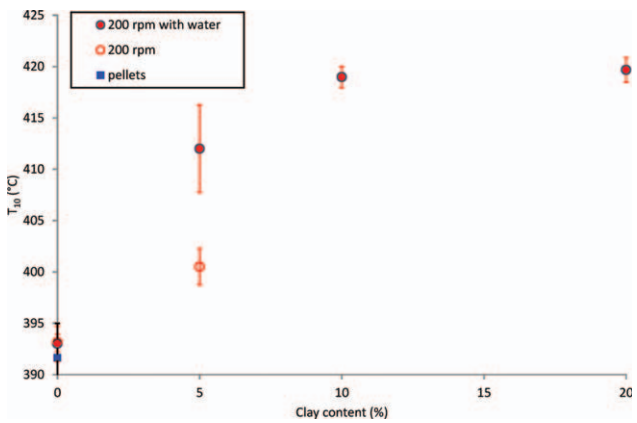

Figure 13. Thermogravimetric analysis of the PA11 nanocomposites. [Color figure can be viewed in the online issue, which is available at wileyonlinelibrary.com.]

appears that T10 is lower for nanocomposites elaborated without water injection. In the same way than for mechanical properties, this is explained by the better dispersion state achieved when water is added. The PA11/NaMMT thermal stability improvement can also be explained by the fact that the dispersed NaMMT layers lead to the activation of a charring effect under thermal attack which leads to a higher degradation temperature.

DISCUSSION

Well-dispersed PA11 nanocomposites may be obtained on the basis nonorganomodified clays using the water-assisted melt blending route. Particularly it has been shown that an exfoliated morphology can be obtained until 10% wt of clay depending on the elaboration conditions. In opposition previous studies reported that 4% wt of clay was the maximum content in order to obtain a fully exfoliated sample. The origin of this apparent contradiction with the results of the literature is twofold. On the one hand it has to be kept in mind that the PA11 used here is an injection grade which means that the molecular mass is relatively low favoring thus the diffusion of the chains into the clay platelets. On the other hand, the main reason at the origin of the good dispersion state achieved is that water is injected during the extrusion process. Regarding to the effect of the processing conditions, the screw speed does not seem to play a major role on the obtained morphology. More precisely, increasing the screw speed does not have the beneficial effect expected. Nevertheless no conclusion can be drawn as the residence time is not the same.

On the other hand this study clearly highlights the positive effect of injecting water on the dispersion state and thus on the resulting properties. Indeed it seems possible via this route to use NaMMT as filler for the elaboration of high performance materials, which is cheaper and greener than modified clay. In this way, in order to definitely prove the efficiency of this method, PA11 nanocomposites based on pristine clay have been elaborated and characterized. Indeed this kind of clay can be considered as the most unfavorable for the achievement of a true nanocomposite as most pollutants are still present into. The observed morphologies of these samples, obtained by means of TEM are reported on Figure 14.

Surprisingly it appears that the pristine clay is well dispersed into the PA11 matrix and that an exfoliated morphology is obtained even for a clay content of 10% wt. This definitely shows the positive effect of water injection during the extrusion. The latter originates from two main reasons which are combined in a synergistic way. On the one hand injected water acts as a surfactant; water molecules easily diffuse between the clay platelets involving an increase of their spaces which causes a decrease of the interactions forces. Thus the polymer chains can easily diffuse into the galleries in order to exfoliate the clay. On the other hand, the combination of water and pressure induces a solubilization of PA11 and thus a drastic increase of the chains' mobility. Beyond this positive effect, the results obtained in this study also underline that the dispersion of the clay into the matrix is primarily governed by thermodynamical and affinity aspects. Indeed even if no water is added during the extrusion the resulting morphology is satisfying meaning that PA11 and MMT have a good affinity. An original result obtained in this study is the morphology of the samples having a clay content of 10% wt at least. Indeed TEM and SAXS analyses have revealed that, in these cases, the isolated platelets were not completely randomly distributed into the sample but they are rather organized in mesoscale domains into which they lies parallel to each other with an almost constant mean distance between them. This kind of behavior is uncommon but may be intuitively explained by the fact that the observed mean distance corresponds to an equilibrium one. Indeed in a given volume of matrix, up to a critical clay content, the clays cannot be distributed so as to be independent from each other, i.e. a "true" exfoliated state cannot be achieved any more. As a consequence, above this critical value the clay platelets interact together and in this way it seems consistent that the most energetically stable dispersion of isolated platelets is not a random dispersion but rather an organized one where the platelets are parallel the one to the others and separated from a given average distance which directly depends of the clay content. As a consequence the dispersion state achieved at high clay loadings can be considered as a nanostructured exfoliated morphology. Finally the structural characterization performed in this study also allows to better understand the origin of the mechanical properties enhancement observed. Indeed such an improvement is not commonly encountered in the case of polymer nanocomposites,

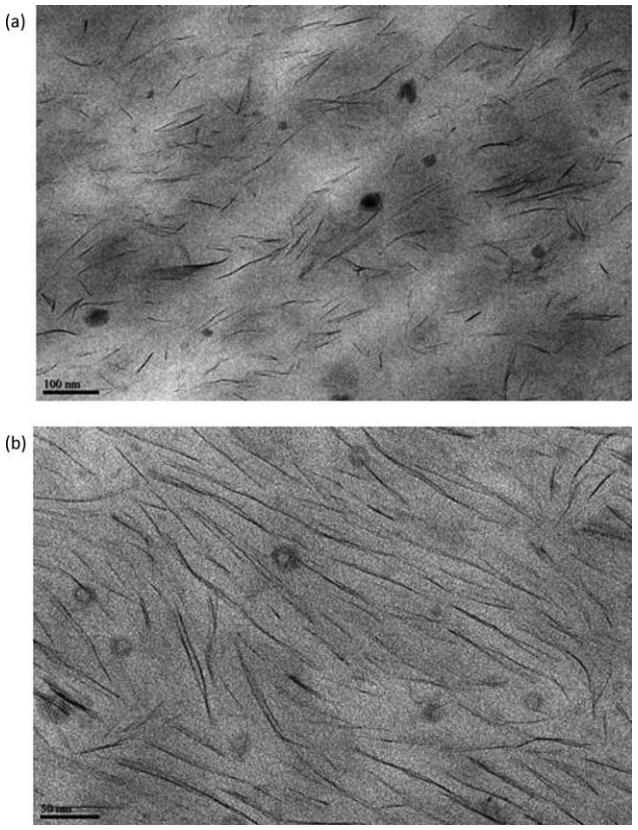

Figure 14. TEM observations of PA11 nanocomposites based on pristine clay filled at (a) 5% wt and (b) 10% wt.

particularly when unmodified clays are used. Beyond the dispersion state, which determines the specific surface of interaction, that's to say the exchange surface between polymer and clay, the properties improvement is also strongly dependent of the interaction degree between the polymer and the clay. This interaction degree depends on the chemical nature of both polymer and clays. Indeed if there's a good affinity between filler and matrix, some bonds can be created involving strong interactions. In the case of PA11 nanocomposites the WAXS study tends to show that there's a strong affinity between the polymer and the clay platelets. On the one hand this is confirmed by the change of the crystalline structure induced by the presence of the clays. Moreover, WAXS results have revealed that the PA11 γ crystals, induced due to the presence of the filler, are lying on the clay platelets surface. It can be assumed that hydrogen bonds may be involved at the interface between the platelets and the crystals, playing the role of linkage. As a consequence the clays directly influence the mechanical behavior of PA11.

CONCLUSION

PA11 nanocomposites based on unorganomodified MMT have been successfully elaborated using the water-assisted extrusion route. The positive effect of injecting water on the resulting morphology has been proved and is explained by the fact that PA11 and water are miscible at high pressure and high temperature. Particularly it has been possible to elaborated well-exfoliated nanocomposites with clay contents as high as 10% wt. Regarding to structural aspects, it has been shown that the presence of the filler infers on the crystalline form induced, particularly it promotes the formation of the more stable crystalline form and it allows to form thicker crystals. Moreover, TEM and SAXS analyses have revealed that from 10% wt of clay, the clay platelets were no more randomly distributed but are rather mesostructurated. Indeed, some nanometer sized domains were platelets are parallel the one to the others can be evidenced.

Various characterization techniques have shown that incorporating clays into PA11 has a beneficial effect on its properties. For example, regarding to mechanical properties, adding 10% wt of filler doubles the value of the Young's modulus, which allows considering the use of PA11 in new applications. Moreover, in addition to this mechanical properties enhancement it can be supposed that the good dispersion state achieved thanks to water-assisted extrusion may also greatly enhance the barrier properties of PA11. Second, the addition of clay drastically enhance the thermal stability of the material by increasing the start of its degradation of 35°C when 10% wt of filler is added and well dispersed. The structural characterization has also allowed to show that in the case of nanocomposites, the PA11 crystals are lying onto the clay platelets. Finally, regarding the influence of the extrusion conditions, it has been shown that in the case of PA11 nanocomposites the residence time has a greater effect on the dispersion degree than the shearing force. This relies in the fact that for long residence times, PA11 macromolecules have the time to diffuse into the clay platelets. In other words, the exfoliation mechanism involved in the case of PA11 nanocomposites differs from the one currently proposed. While in most cases it is the shearing force that induced the delamination of the stacked clay platelets, and thus which is the driving force, for PA11 nanocomposites it is rather the diffusion of the macromolecules into the clay galleries that induced their delamination and thus which governs the exfoliation process.

ACKNOWLEDGMENTS

Authors thank P. Lipnik and P. Vanvelthem for their technical support. Financial support from Region Nord Pas de Calais and European FEDER for the SAXS/WAXS equipment is also gratefully acknowledged.

REFERENCES

1. Kojima, Y.; Usuki, A.; Kawasumi, M.; Okada, A.; Fukushima, Y.; Kurauchi, T.; Kamigaito, O. J. *Mater. Res.* **1993,** *8*, 1185.
2. Kojima, Y.; Usuki, A.; Kawasumi, M.; Okada, A.; Kurauchi, T.; Kamigaito, O. J. *Polym. Sci. Part A: Polym. Chem.* **1993,** *31*, 983.
3. Usuki, A.; Kojima, Y.; Kawasumi, M.; Okada, A.; Fukushima, Y.; Kurauchi, T.; Kamigaito, O. J. *Mater. Res.* **1993,** *8*, 1179.
4. Liu, L.; Qi, Z.; Zhu, X. J. *Appl. Polym. Sci.* **1999,** *71*, 1133.
5. Cho, J. W.; Paul, D. R. *Polymer* **2001,** *42*, 1083.
6. Reichert, P.; Kressler, J.; Thomann, R.; Mülhaupt, R.; Stöppelmann, G. *Acta. Polym.* **1998,** *49*, 116.
7. Kim, G. -M.; Lee, D. -H.; Hoffmann, B.; Kressler, J.; Stöppelmann, G. *Polymer* **2001,** *42*, 1095.
8. Kojima, Y.; Usuki, A.; Kawasumi, M.; Okada, A.; Kurauchi, T.; Kamigaito, O. J. *Appl. Polym. Sci.* **1993,** *49*, 1259.
9. Gilman, J. W. *Appl. Clay Sci.* **1999,** *15*, 31.
10. Mathias, L. J.; Davis, R. D.; Jarrett, W. L. *Macromolecules* **1999,** *32*, 7958.
11. Wu, G.; Yano, O.; Soen, T. *Polym. J.* **1986,** *18*, 51.
12. Mathur, S. C.; Sent, A.; Newman, B. A.; Scheinbeim, J. I. *J. Mater. Sci.* **1988,** *23*, 977.
13. Takase, Y.; Lee, J. W.; Scheinbeim, J. I.; Newman, B. A. *Macromolecules* **1991,** *24*, 6644.
14. Werth, M.; Hochstetter, G.; Dang, P.; Chedozeau, N. *Proc. Int. Conf. Offshore Mech. Arctic Eng.* **2002,** *3*, 449.
15. Peppin, A. *ANTEC Conf. Proc.* **1998,** *3*, 2759.
16. Smith, W. C. *Tech. Text. Int.* **1996,** *5*, 15.
17. Vogdes, C. Crosslinked, Heat Stable Nylons 11 and 12 for Use in the Automotive Industry. Paper presented at the National Technical Conference—Society of Plastics Engineers; **1983;** p 144–147.
18. Formes, T. D.; Paul, D. R. *Macromolecules* **2004,** *37*, 7698.
19. Chen, P. K.; Newman, B. A.; Scheinbeim, J. I.; Pae, K. D. *J. Mater. Sci.* **1985,** *20*, 1753.
20. Rhee, S.; White, J. L. *J. Polym. Sci. Part B: Polym. Phys.* **2002,** *40*, 1189.
21. Rhee, S.; White, J. L. *J. Polym. Sci. Part B: Polym. Phys.* **2002,** *40*, 2624.
22. Rhee, S.; White, J. L. *Polym. Eng. Sci.* **2002,** *42*, 134.

23. Hu, G.; Ding, Z.; Li, Y.; Wang, B. J. *Polym. Res.* **2009,** *16*, 263.
24. Li, Y.; Hu, G.; He, B. *e-Polymers* **2011, 60.**
25. Li, Y.; Hu, G.; Tang, W.; Wang, Z.; Xie, J. *Polym. Mater. Sci. Eng.* **2006,** *22*, 172.
26. Li, Y.; Huo, G.; He, B. *Adv. Mater. Res.* **2011,** *150*, 223.
27. Huang, S.; Wang, M.; Liu, T.; Zhang, W.; Tjiu, W. C.; He, C.; Lu, X. *Polym. Eng. Sci.* **2009,** *49*, 1063.
28. Lao, S. C.; Wu, C.; Moon, T. J.; Koo, J. H.; Morgan, A.; Pilato, L.; Wissler, G. J. *Compos. Mater.,* **2009,** *43*, 1803.
29. Mago, G.; Kalyon, D. M.; Fisher, F. T. *J. Polym. Sci. Part B: Polym. Phys.* **2011,** *49*, 1311.
30. Sonawane, S. S.; Mishra, S.; Shimpi, N. G. *Polymer* **2009,** *48*, 1055.
31. Yang, Z.; Huang, S.; Liu, T. J. *Appl. Polym. Sci.* **2011,** *122*, 551.
32. Zhang, Q.; Yu, M.; Fu, Q. *Polym. Int.* **2004,** *53*, 1941.
33. Zhang, Y.; Wang, B.; Hu, G. J. *Appl. Polym. Sci.* **2012,** *123*, 273.
34. Zhang, Y.; Hu, G.; Wang, B. *e-Polymers* **2011,** 48.
35. Liu, T.; Lim, K. P.; Tjiu, W. C.; Pramoda, K. P.; Chen, Z. -K. *Polymer* **2003,** *44*, 3529.
36. Hu, Y.; Shen, L.; Yang, H.; Wang, M.; Liu, T.; Liang, T.; Zhang, J. *Polym. Test.* **2006,** *25*, 492.
37. Bur, A. J.; Roth, S. C.; Start, P. R.; Lee, Y. -H.; Maupin, P. H. *Trans. Inst. Meas. Control* **2007,** *29*, 403.
38. Touchalaume, F.; Soulestin, J.; Sclavons, M.; Devaux, J.; Lacrampe, M. F.; Krawczak, P. *Polym. Degrad. Stab.* **2011,** *96*, 226.
39. Touchaleaume, F.; Soulestin, J.; Sclavons, M.; Devaux, J.; Cordenier, F.; van Velthem, P.; Flat, J. J.; Krawczak, P. *Express Polym. Lett.* **2011,** *5*, 1085.
40. Fedullo, N.; Sclavons, M.; Bailly, C.; Lefebvre, J. -M.; Devaux, J. *Macromol. Symp.* **2006,** *233*, 235.
41. Fedullo, N.; Sorlier, E.; Sclavons, M.; Bailly, C.; Lefebvre, J. -M.; Devaux, J. *Prog. Org. Coat.* **2007,** *58*, 87.
42. Verlet, J.; Cavaille, J. Y.; Perez, J. J. *Polym. Sci. Part B: Polym. Phys.* **1990,** *28*, 2691.
43. Baschek, G.; Hartwig, G.; Zahradnik, F. *Polymer* **1999,** *40*, 3433.
44. Papir, Y. S.; Kapur, S.; Rogers, C. E. *J. Polym. Sci. Part A-2: Polym. Phys.* **1972,** *10*, 1305.
45. Wevers, M. G. M.; Mathot, V. B. F.; Pijpers, T. F. J.; Goderis, B.; Groeninckx, G. *Lecture Notes Phys.* **2007,** *714*, 151.
46. Wevers, M. G. M.; Pijpers, T. F. J.; Mathot, V. B. F. *Thermochim Acta.* **2007,** *453*, 67.
47. Charlet, K.; Mathot, V.; Devaux, J. *Polym. Int.* **2011,** *60*, 119.
48. Bousmina, M. *Macromolecules* **2006,** *39*, 4259.
49. Lecouvet, B.; Sclavons, M.; Bourbigot, S.; Devaux, J.; Bailly, C. *Polymer* **2011,** *52*, 4284.
50. Zhang, Q.; Mo, Z.; Zhang, H.; Liu, S.; Cheng, S. Z. D. *Polymer* **2001,** *42*, 5543.
51. Zhang X.; Yang, G.; Lin, J. J. *Appl. Polym. Sci.* **2006,** *102*, 5483.
52. VanderHart, D. L.; Asano, A.; Gilman, J. W. *Chem. Mater.* **2001,** *13*, 3781.
53. Liu, T. X.; Liu, Z. H.; Ma, K. X.; Shen, L.; Zeng, K. Y.; He, C. B. *Compos. Sci. Tech.* **2003,** *63*, 331.
54. Fornes, T. D.; Paul, D. R. *Macromolecules* **2004,** *37*, 7698.